Effects of laser peening on fretting wear behaviour of alloy 718 fretted against two different counterbody materials

S Anand Kumar[1,2], R Sundar[3], S Ganesh Sundara Raman[4], R Gnanamoorthy[5], R Kaul[6], K Ranganathan[3] and K S Bindra[3]

Abstract

This paper deals with the effects of laser peening on fretting wear behaviour of a nickel-based superalloy, alloy 718, fretted against two different counterbody materials (alumina and SAE 52100 steel). Laser peening was carried out on alloy 718. Microstructural characterization of laser peened surface was done by electron back-scattered diffraction and transmission electron microscopy. Surface roughness, nanoindentation hardness, and residual stress of both laser peened and unpeened samples were determined. Fretting wear tests were conducted on unpeened and laser peened samples using two different counterbody materials (alumina and SAE 52100 steel balls). The results show that nanocrystallites formed in the surface and near-surface regions and compressive residual stress were induced after laser peening. Hardness increased due to grain refinement at the surface and near-surface regions. There was no significant change in the surface roughness. The laser peened sample exhibited lower tangential force coefficient values compared to unpeened samples at all loads, which may be attributed to higher hardness. Samples fretted against alumina counterbody exhibited higher tangential force coefficient compared to samples fretted against steel counterbody. Owing to increased surface hardness and higher compressive residual stress, laser peened samples exhibited lower fretting wear damage compared to unpeened samples. Due to tribochemical reactions, the wear volume of unpeened and laser peened samples fretted against alumina counterbody was higher than that of the samples fretted against steel counterbody.

Introduction

Alloy 718 is a nickel-based superalloy, principally developed for elevated temperature applications for aerospace industries. It exhibits good strength, excellent creep resistance at elevated temperatures, and superior oxidation resistance.[1] However, its wear resistance has been reported to be poor,[2] and this needs to be addressed for prospective tribological applications. Fretting wear is a type of wear due to relative tangential motion experienced by contacting bodies resulting from vibration or cyclic loading. It leads to disastrous failures in many components/parts.[3] Based on the magnitude of applied stresses and the amplitude of displacement, damage mechanisms such as formation and ejection of debris at the tribo-interface or crack nucleation and propagation will take place.[4] So fretting damage should be considered as an important factor in the design of joints working under fretting conditions.

It is known that the presence of work-hardened surface layer and surface compressive residual stresses would improve the tribological and fatigue properties. It could be accomplished by an appropriate surface engineering technique, such as ball burnishing,[5] shot

[1]Department of Mechanical Engineering, ACS College of Engineering, Bengaluru, India
[2]Department of Mechanical Engineering, School of Engineering, Dayananda Sagar University, Bengaluru, India
[3]Solid State Laser Division, RRCAT, Indore, India
[4]Department of Metallurgical and Materials Engineering, IIT Madras, Chennai, India
[5]Indian Institute of Information Technology Design and Manufacturing, Chennai, India
[6]Laser Material Processing Division, RRCAT, Indore, India

Corresponding author:
S Anand Kumar, Department of Mechanical Engineering, School of Engineering, Dayananda Sagar University, Bengaluru 560068, Karnataka, India.
Email: anandkumarait@gmail.com

peening,[6] ultrasonic nanocrystal surface modification (UNSM),[7] ultrasonic shot peening (USSP),[8] machine hammer peening,[9] detonation gun spraying,[10] plasma assisted nitriding,[11] surface mechanical attrition treatment (SMAT),[12] etc. which have been successfully employed on alloy 718 samples.

There have been studies on the tribological properties of surface-engineered alloy 718. Kim et al.[13] studied the seizure characteristics of UNSM-treated alloy 718. Their results showed that the UNSM-treated samples had improved tribological properties compared to the untreated samples owing to increased surface hardness and compressive residual stress introduced by UNSM treatment. Varshni Singh and Meletis[14] carried out nitriding process at low temperature by intensified plasma-assisted processing on alloy 718 samples. They found superior wear resistance of nitrided samples due to higher hardness of the nitrided surface layer. Hirschmann et al.[15] investigated the influence of plasma immersion ion implantation (PIII) technique on the tribological properties of alloy 718. They found that nitrogen PIII treatment done for 3 h resulted in significant improvements in wear resistance and reduction in the friction coefficient. Kovacı et al.[16] studied the effect of plasma nitriding treatment on friction behaviour of alloy 718. The plasma nitriding significantly decreased friction coefficient and the effect was dependent on the nitriding time and temperature.

There are a few studies on the fretting wear behaviour of surface-modified alloy 718 available in the open literature. Amanov et al.[7] studied the influence of UNSM treatment on the fretting wear resistance of alloy 718 at various temperatures. They used bearing steel ball as counterbody during fretting tests. They reported that the UNSM-treated samples exhibited lower friction coefficient and enhanced fretting wear resistance compared to the untreated ones. It was attributed to the fine grain structure and higher surface hardness. Anand Kumar et al.[12] have investigated the effect of SMAT treatment and its duration on the fretting wear behaviour of alloy 718 samples. SMAT was performed for 30 and 60 min. They employed alumina ball as the counterbody during fretting wear tests. Their results showed higher fretting wear resistance and lower tangential friction coefficient for the SMAT-treated sample for 30 min compared to untreated samples, due to an optimum combination of hardness and toughness of the treated samples. On the other hand, the samples treated for 60 min had inferior fretting wear resistance compared to untreated samples, owing to the higher hardness and reduced toughness.

In the present work, laser peening is employed as a surface engineering technique. In laser peening, an intense laser pulse is used to produce shockwaves, which result in strain hardening, improved hardness and compressive residual stress at the surface. This surface treatment is known to modify the microstructure at and near the surface leading to grain refinement with high density arrays of dislocations.[17] Laser peening is capable of introducing compressive residual stresses below surface to a larger depth compared to shot peening. The thermal stability of residual stresses induced by laser peening has been reported to be superior owing to the less amount of near surface work hardening.[18] This is an important property for high temperature applications, e.g. low-pressure compressor disks and blades of aircraft engines. Laser peening has been shown to improve hardness and fatigue strength in a number of metallic materials including nickel based superalloys.[19–22] Laser peening does not change the surface finish much, which is more important for the improvement of fatigue properties.[23]

The studies on laser peened nickel-based superalloys either focus on improvement of the fatigue resistance or thermal stability of the induced compressive residual stress. To the best of the authors' knowledge, the effect of laser peening on the fretting wear behaviour of alloy 718 has not been reported. The present paper attempts to study the effect of laser peening on microstructure and fretting wear behaviour of alloy 718. As fretting wear process is strongly influenced by counterbody materials, it is important to understand the influence of counterbody material on fretting wear behaviour so that efficient and reliable engineering systems with better fretting wear resistance can be built. Alumina and SAE 52100 steel were used as counterbody materials.

Experimental procedure

The material used in the present study is alloy 718 in standard double-aged condition with hardness of 435 $H_{v0.1}$. Laser peening was done on coupons of size $80 \times 10 \times 6$ mm^3. A PVC-based black insulation tape,[24] which served as the sacrificial coating, was used during laser peening. The laser system used was an oscillator–amplifier-based in-house developed high-energy flash lamp-pumped electro-optically Q-switched Nd:YAG laser system giving an output of 2.5 J at a repetition rate of 5 Hz with a spot diameter of 9 mm ($1/e^2$ points) and a pulse width $<$10 ns.[25] A lens of 400 mm focal length was used to focus the laser beam to the target. Target was placed well ahead of the focal plane, since the intensity at the focal plane would be adequate to create air breakdown and hence the laser energy may be efficiently used in creating shock wave for peening. Laser peening parameters are listed in Table 1.

Table 1. Laser peening parameters used in the present study.

Pulse energy (J)	Pulse width (ns)	Laser spot diameter (mm)	Pulse repetition rate (Hz)	Laser scan rate (mm/s)	Track-to-track displacement (mm)
1.4	7	1.8	2	1.7	0.7

Samples for electron back-scattered diffraction (EBSD) analysis were polished following the standard procedure used in metallography and colloidal silica was used for final polishing. The microstructure was observed across cross section moving from the peened surface to base metal. For EBSD analysis, a scanning electron microscope (SEM) (Philips, FEI Quanta 200) operating at 30 kV was used. The step size used was 750 nm. A transmission electron microscope (TEM) (Philips, CM 12) operating at 120 kV was used for microstructural characterization. Using a low speed diamond saw cutting machine, thin foils of the laser peened sample were cut along the direction parallel to the peened surface. The side opposite to the peened surface of the foil was mechanically polished to about 100 μm thickness. This was followed by dimpling and finally ion milling was done to obtain electron transparency. X-ray diffraction (XRD) was done on the surface of unpeened and laser peened samples using an X-ray diffractometer (Bruker, D8 Discover, Madison, USA) with Cu K_α radiation at a scanning rate of 1 step/s and step size of 0.03°/step. An optical surface profilometer (Wyko, NT8000) was used to evaluate the surface morphology and surface roughness of unpeened and laser peened samples. A nanoindenter (Hysitron, Triboscope TI 950) was employed to determine nanoindentation hardness just below the peened surface at a load of 10 mN. Trapezoidal load profile was employed with a loading rate of 1.25 mN/s, a dwell time of 2 s and an unloading rate of 2 mN/s. One measurement was made in each sample due to limitation in the resources. The residual stresses in unpeened and laser peened samples were determined using a stress analysis system (Proto Manufacturing, iXRD) with Cu K_α radiation ($\lambda = 1.54$ A°). The standard deviation versus $\sin^2\psi$ technique suggested by Cullity[26] and Noyan and Cohen[27] was followed.

Samples of size $10 \times 10 \times 6$ mm^3 were cut from the peened coupons and used for fretting wear tests. For comparison, unpeened specimens were also tested. The details of the in-house developed fretting wear test rig are given elsewhere.[28] Fretting wear tests were conducted at different normal loads (1.96, 4.9, 9.8, 14.7, and 19.6 N) with a constant displacement of 55 μm and a frequency of 5 Hz. The different normal loads were chosen so as to obtain different fretting regimes viz. gross slip, mixed stick–slip and stick. Two different counterbody materials (alumina and SAE 52100 steel) were used. They were in the form of balls of 10 mm diameter. Properties of the counterbody materials are listed in Table 2. All fretting wear

tests were conducted up to 50,000 cycles in laboratory ambience (humidity of $80 \pm 5\%$ and temperature of 303 ± 5 K). For each condition and at each normal load, one test was conducted due to limitation in the resources. Friction force (tangential force) and displacement were acquired at regular time intervals using a data acquisition system. Friction loops were drawn with tangential force on the y-axis and the imposed displacement on the x-axis. Tangential force coefficient (TFC) was calculated by dividing half of the difference between maximum and minimum tangential force obtained in a friction loop with the corresponding normal load. Using the SEM, observations on fretting wear scars in the tested samples were made and the size of the scar was measured along directions parallel and perpendicular to the fretting direction. Subsequently, calculations of fretting wear volume were performed using equations derived by Kalin and Vizintin.[29] Also, wear rate was computed by dividing the wear volume by normal load and displacement. Energy-dispersive X-ray spectroscopy (EDS) was employed to characterize the fretted counterbody samples.

Initial maximum Hertzian contact pressures (P) and initial contact radius (a) were computed using equations (1) to (3). By assuming the interaction between normal stress and the traction force due to difference in elastic constants of the two solids is negligible, the contact pressure between the counterbody (alumina or steel) with a normal load (N) and sliding over a flat specimen is given by Hertz theory[30].

$$P = \left(\frac{6\,N\,E^{*2}}{\pi^3 r^2} \right)^{\frac{1}{3}} \qquad (1)$$

$$\frac{1}{E^*} = \frac{(1 - \gamma_1^2)}{E_1} + \frac{(1 - \gamma_2^2)}{E_2} \qquad (2)$$

$$a = \left(\frac{3\,N\,r}{4\,E^*} \right)^{\frac{1}{3}} \qquad (3)$$

E_1 and γ_1 are the elastic modulus and Poisson's ratio of flat specimen (unpeened or laser peened sample), respectively, E_2 and γ_2 are the elastic modulus and Poisson's ratio of counterbody material (alumina or steel), respectively, E^* is the composite elastic modulus, and r is the radius of the ball (5 mm).

Results and discussion

Microstructure, surface roughness, hardness and residual stress

Cross-sectional EBSD inverse pole figures and image quality maps of alloy 718 samples before and after laser peening are shown in Figure 1. For the employed laser peening parameters, the micrographs shown in Figure 1(c) and (d) do not indicate any noticeable

Table 2. Properties of counterbody materials.

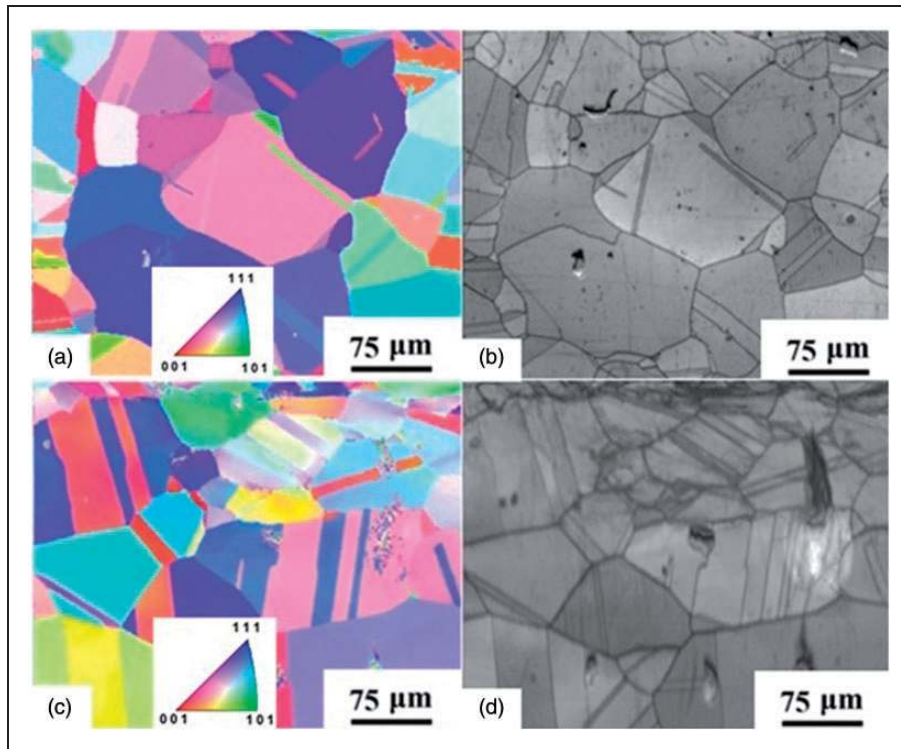| Material	Hardness (H_V)	Elastic modulus (GPa)	Poisson's ratio
SAE 52100 steel	830	210	0.29
Alumina	1950	382	0.24

Figure 1. Electron backscattered diffraction micrographs of alloy 718 samples: (a) and (b) unpeened; (c) and (d) laser peened; (a) and (c) are inverse pole figure maps and (b) and (d) are corresponding image quality maps.

changes in the microstructure in the near surface region after laser peening compared to unpeened samples (Figure 1(a) and (b)). It may be noted that SMAT done on the same material alloy 718 resulted in severe plastic deformation in the surface and near-surface regions and the thickness of the severe plastic deformed layer was about 200 μm.[12] The absence of a significant plastic deformation zone in case of laser peened sample in the near surface region in the present study could be attributed to a very short time of interaction between the high pressure shock wave and the sample, about 0.05 μs, which is roughly 10 times lower compared to conventional shot peening process. This is similar to the result reported by Gill et al.[31]

Figure 2 shows X-ray diffraction patterns obtained in the samples in the unpeened and laser peened conditions. The XRD pattern of the laser peened sample is similar to that of the unpeened sample. It was expected that the laser peened sample would exhibit peak broadening in its XRD pattern. It is known that broadening of diffraction peaks is attributed to lattice distortion, caused by higher level of cold work resulting in a decrease in grain size and increase in the microstrain. The absence of peak broadening in the laser peened sample could be attributed to lesser extent of lattice distortion and work hardening. It may be noted that the mean penetration depth of X-rays in alloy 718 is about 8 μm. So the XRD results correspond to sub-surface coarse grains. From this it may be presumed that the thickness of severe plastically deformed zone with very fine
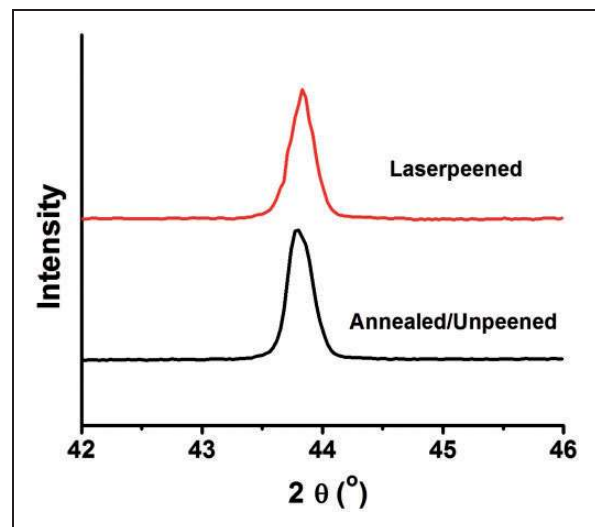

Figure 2. XRD patterns of alloy 718 in two conditions.

grain structure (if developed) to be less than 8 μm in alloy 718.

Figure 3(a) shows a dark field transmission electron micrograph of a laser peened sample and Figure 3(b) shows its selected area electron diffraction (SAED) pattern. The dark field image reveals the formation of nanocrystallites. The SAED pattern shows spotted ring pattern, indicating the formation of nanocrystalline structure. The average crystallite size is found to be 13 nm in the laser peened sample.

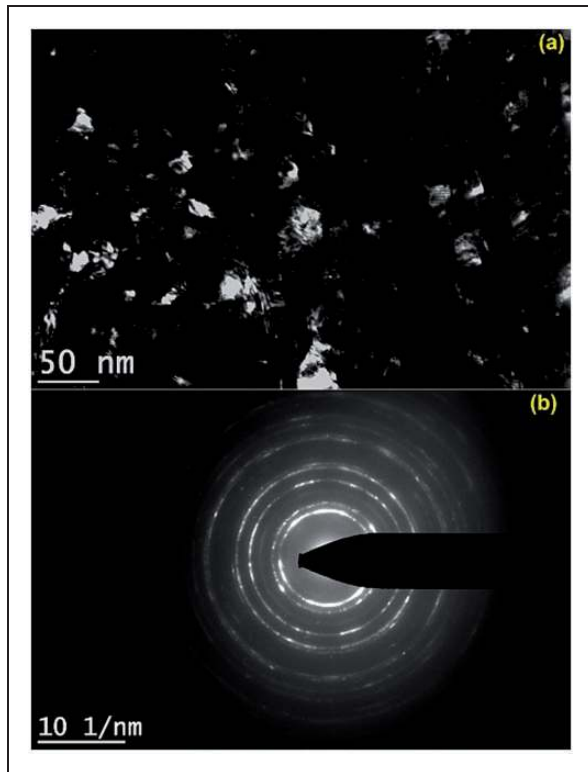**Figure 3.** Transmission electron micrograph (a) of the surface layer of laser peened alloy 718 and corresponding SAED pattern (b).

Figure 5. Surface morphology of alloy 718 samples: (a) unpeened and (b) laser peened.
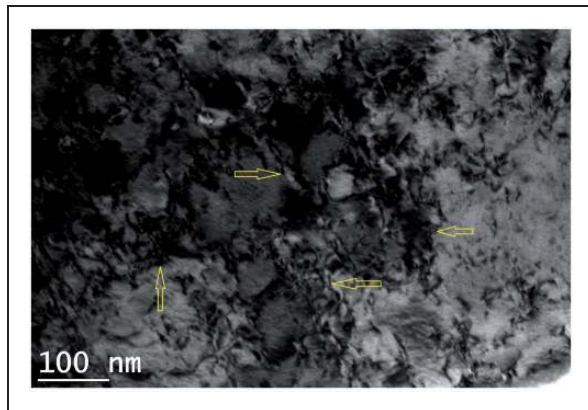

Figure 4. Transmission electron micrograph of near-surface region of laser peened alloy 718 showing the presence of dislocation tangles as indicated by arrows.

The average grain size of unpeened sample is 94 μm. They corroborate the nanostructured surface formation due to laser peening. Such a significant reduction in grain size achieved through surface nanocrystallization by laser peening is comparable to that imparted by surface severe plastic deformation processes such as USSP[8] and SMAT.[12] The shock wave leads to deformation at high strain rates and produces a large number of dislocations in alloy 718. The induced plastic strain is accommodated by dislocation networks f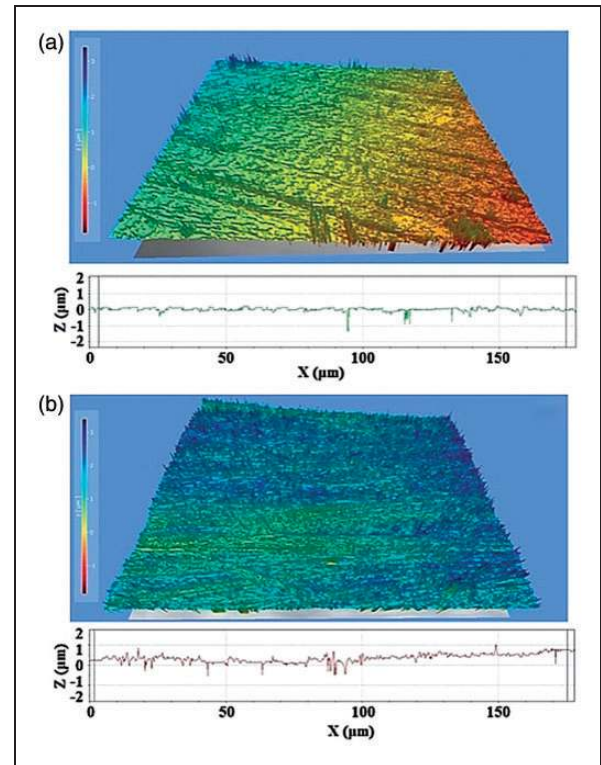ormed by rearrangement and annihilation of dislocations resulting in the formation of nanocrystallites.[32] Bugayev et al.[33] have reported occurrence of nanocrystallization on the laser peened surface of alloy 600. Formation of nanocrystallites by laser peening has also been reported in aluminum alloy,[34] austenitic stainless steel,[35] Ti-6Al-4 V,[36] etc. It may be noted that the foils for transmission electron microscopy were prepared from the top surface layer of laser peened sample with the thickness not exceeding 5 μm and so the presence of nanocrystallites could be observed. On the other hand, XRD results could not indicate the presence of nanocrystallites as the penetration depth of X-rays in alloy 718 is about 8 μm and so XRD results correspond to sub-surface coarse grains.

Figure 4 shows dislocation tangles just below the laser peened surface, which might have been produced by shock waves. Similar dense dislocation arrangements have been reported by Nalla et al.[7] in the near-surface regions of laser peened Ti-6Al-4 V. Such dislocation tangles would aid in grain refinement resulting in development of nanostructured surface layer.[37]

Figure 5 shows the surface morphologies of unpeened and laser peened samples. There is no significant change in surface topography due to laser peening. There was a slight increase in surface roughness (see Table 3). During laser peening, the shock waves with higher magnitude of peak pressure are responsible for inducing the plastic deformation

together with the generation of dimples on the surface of metallic materials. The formed dimples on the material's surface would pileup on the edges. Subsequently, the pileups induced by the shockwaves will be flattened by adjacent laser impact.[31] Due to this, laser peening does not alter the surface roughness significantly.

Figure 6 shows the typical nanoindentation load–displacement (penetration depth) profiles of laser peened and unpeened samples. The area bounded by loading and unloading curves is defined as plastic deformation work (W_P) and it could indicate the degree of resistance to plastic deformation and the wear resistance.[36] Laser peened sample revealed lesser plastic deformation work compared to unpeened sample, signifying its relatively better resistance to plastic deformation and therefore enhanced wear resistance.

In case of the laser peened sample and unpeened sample subjected to the same load of 10 mN, the indenter penetrated to a depth of 240 nm and 314 nm, respectively. The relatively lower depth of penetration in the laser peened sample could be attributed to the enhanced hardness and compressive residual stress introduced by laser peening (see Table 3). Zhu et al.[38] explained the influence of the nature of residual stresses on the load–depth curve obtained by nanoindentation technique for the same value of maximum depth in the case of (100) copper single crystal. They observed lesser load for tensile residual stressed sample and higher load for compressive residual stressed sample compared to unstressed sample for the same value of maximum depth. As the indentation stress acts normal to the sample surface, the direction of contact shear stress underneath the indenter is the same as with the tensile residual stress direction. Hence, the tensile residual stress enhanced the amount of shear stress compared to that in the unstressed samples. The increased shear stress in the case of tensile residual stressed sample can increase the plastic deformation due to indentation. Hence, lesser load was required compared to the unstressed state for the same indentation depth. The converse was true regarding the influence of compressive residual stress. They reported that the nature of residual stress had a significant impact on the shapes of the loading curves. The loading curve for the sample with compressive residual stress had higher slope and shifted leftward compared to unstressed state. On other hand, in the case of the sample with tensile residual stress, the loading curve had a lower slope and shifted on the right side compared to unstressed state. In the present study, the peened sample exhibits a lower penetration depth of 240 nm for the same maximum load and its loading curve is on the left side of the unpeened sample's loading curve. From this, it may be said that laser peening process induced compressive residual stress in the surface layers of alloy 718, which is confirmed by the residual stress values determined using XRD stress analyzer (Table 3).

Figure 7 shows the nanoindentation hardness profile across the cross section of a laser peened sample. The increase in surface hardness is due to compressive residual stress and grain refinement[39] in the peened surface layer. Beyond about 300 μm depth from the surface, the laser peening did not result in a significant difference in hardness value (Figure 7).

Table 3. Surface roughness, plastic deformation work (W_P) and residual stress of unpeened and laser peened samples.

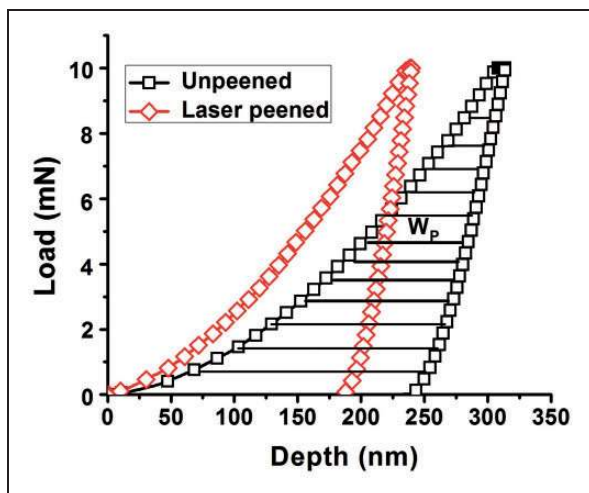|	Surface roughness (μm)		W_P (mJ)	Surface hardness (GPa)	Residual stress (MPa)
	R_a	R_{max}			
Unpeened	0.11	0.95	0.9	4.23	−207
Laser peened	0.33	3.00	0.7	6.71	−605

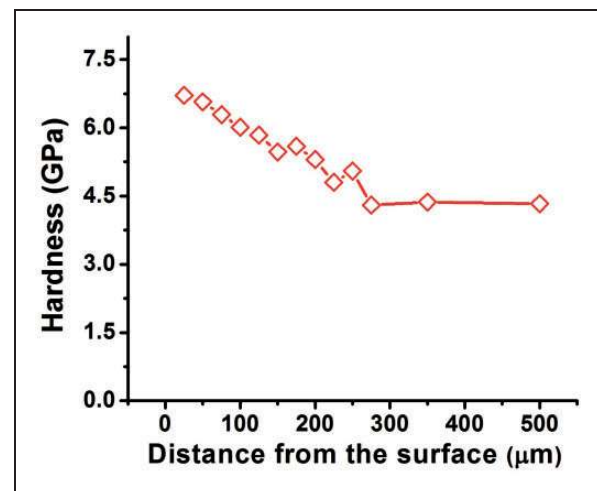**Figure 6.** Load–displacement curves of laser peened and unpeened alloy 718.

Figure 7. Variation of hardness with distance from surface of laser peened alloy 718.

Fretting wear behaviour

Friction loops. A friction loop shows the variation of friction force with imposed displacement corresponding to a fretting cycle. Figure 8 shows the effect of normal load on friction loops corresponding to 10,000[th] cycle for laser peened samples. The shape of loop specifies the type of fretting regime that is operating for a particular normal load. The following regimes were observed – gross slip at 1.96 N, mixed stick–slip at 9.8 N, and near stick at 19.6 N. At the load of 1.96 N, a quasi rectangular loop was formed, which signifies the occurrence of gross slip regime, during which slip occurs in the complete contact region. When the normal load was increased to 9.8 N, it changed to mixed stick–slip regime, which is described by an elliptical shape. During this, part of the displacement between the tribo-surfaces is contained by elastic deformation of the asperities. At 19.6 N normal load, near stick regime is observed, where the applied displacement is accommodated by elastic deformation of the asperities and the loop appears as a straight line. Specimens tested against steel counterbody exhibited lower tangential force compared to those tested against alumina counterbody. It can be attributed to difference between the contact pressure exerted by alumina and steel counterbody on alloy 718 samples (see Table 4). It can be seen that friction force increased as the applied normal load increased – a similar trend has been reported for unpeened and laser peened Ti-6Al-4V.[36]

Tangential force coefficient. Figure 9 shows the variation in TFC of samples fretted against both steel and alumina counterbodies with fretting cycles. The TFC values increased progressively during the initial stage of about 2000 fretting cycles and reached a steady-state condition. The laser peened samples showed lower TFC compared to the unpeened samples at all loads. The relatively lower TFC is due to higher surface hardness of laser peened samples, which can reduce the adhesion during fretting.[40]

It is well known that real contact area is inversely proportional to the hardness of the softer sample of a tribo-pair. Thus laser peened samples with higher hardness (due to grain refinement) will have smaller real contact area. It has also been reported that the nanocrystalline metals and alloys have lower friction coefficient compared to coarse grained metals and alloys,[41] which may be attributed to high hardness.

The samples fretted against steel counterbody had lower TFC values compared to samples fretted against alumina counterbody. This may be attributed to lower Hertzian contact stress induced and smooth surface of the steel counterbody. Alumina counterbody with a rough surface (as seen in the Figure 10
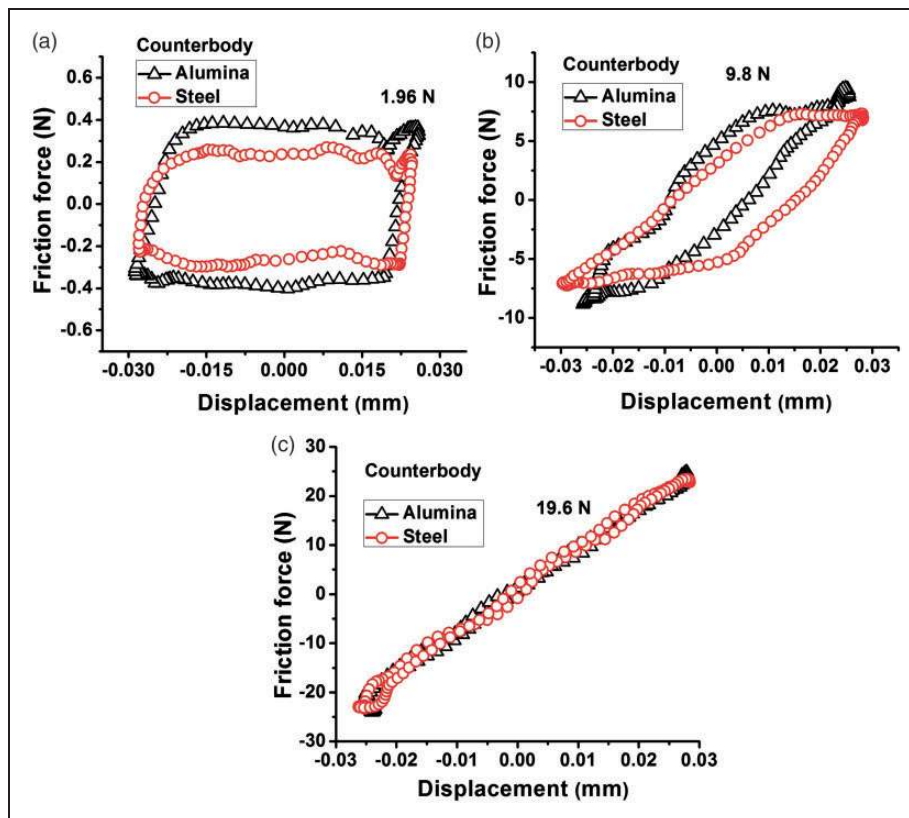

Figure 8. (a to c) Friction force vs. displacement loops corresponding to laser peened samples fretted against steel and alumina counterbodies at three different normal loads after 10,000 cycles.

Table 4. Initial values of maximum contact pressure (P) and contact radius (a) calculated for unpeened and laser peened alloy 718 samples fretted against alumina and steel counterbodies.

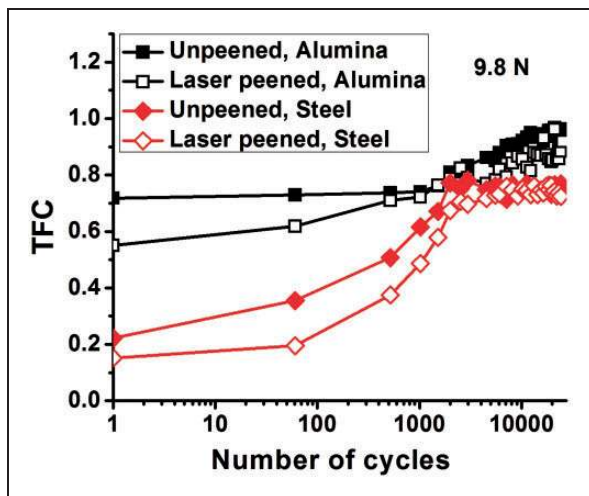| Normal load (N) | Unpeened alloy 718 fretted with | | | | Laser peened alloy 718 fretted with | | | |
| | Alumina | | Steel | | Alumina | | Steel | |
	P (MPa)	a (μm)	P (MPa)	a (μm)	P (MPa)	a (μm)	P (MPa)	a (μm)
1.96	688	37.0	583	41.0	718	36.0	602	39.0
4.90	934	50.0	791	54.0	975	49.0	817	54.0
9.80	1177	63.0	996	69.0	1228	62.0	1030	67.0
14.7	1344	72.0	1138	78.0	1403	70.5	1176	77.0
19.6	1483	79.5	1255	86.0	1547	78.0	1297	85.0

Figure 9. Variation of TFC with the number of fretting cycles for unpeened and laser peened samples fretted against steel and alumina counterbodies.

(a)), the ability to undergo tribochemical reaction (explained in the Fretting wear scars, wear volume and wear rate section), and higher hardness of value of 1950 H_V can result in a higher Hertzian contact stress (see Table 4) in comparison with the steel counterbody with a smooth surface (as seen in the Figure10(b)) and hardness value of 830 H_V. A similar trend has been reported for unnitrided and nitrided Ti-6Al-4V samples.[42]

Fretting wear scars, wear volume, and wear rate. Figure 11 shows the appearance of fretting scars on alloy 718 samples tested against alumina (Figure 11(a) and (b)) and steel (Figure 11(c) and (d)) counterbodies at a normal load of 9.8 N. From the micrographs, the size of scar was measured and fretting volume and wear rate were calculated. Figure 12 shows the variation of wear volume and wear rate of laser peened and unpeened samples fretted against two different counterbodies at different normal loads. Wear volume increased with an increase in the normal load from 1.96 N to 4.9 N due to gross slip condition.

However, it reduced at a normal load of 9.8 N, due to the change in the fretting regime to mixed stick–slip regime. For uncoated steels, a decrease in wear volume with the change in fretting regime from gross slip to mixed stick–slip regime has been observed.[43] A similar trend has been reported for unpeened and laser peened Ti-6Al-4V.[36]

Laser peened samples exhibited lower wear volume and wear rate compared to unpeened samples fretted against both steel ball and alumina ball as shown in Figure 12. This can be attributed to higher surface hardness, lower TFC values, compressive residual stress and less plastic deformation work of laser peened samples. It is well established that harder materials generally exhibit superior fretting wear resistance.[40] The superior fretting wear resistance could be achieved through the harder nanocrystalline surface layer obtained from the laser peening due to the grain refinement at the surface. The laser peening increased the surface hardness from 4.23 GPa to 6.71 GPa (∼59% enhancement) and reduced adhesion resulting in lower TFC. The lower TFC values would contribute towards lowering the magnitude of cyclic tensile shear stresses at the tribo–pair interface leading to enhanced fretting wear resistance.[40]

Furthermore, wear debris generation is coupled with the crack initiation and propagation. The beneficial effect in inhibiting the crack initiation and propagation could be achieved due to the presence of compressive residual stress. Hence, higher the magnitudes of compressive residual stress in the sample, superior will be the tribological properties. It is shown that the existence of compressive residual stress at the surface resulted in lower wear compared to the surface with tensile residual stress.[44] The beneficial effect of the compressive residual stress induced by surface engineering techniques such as shot peening, USNM, SMAT and ion-beam-enhanced deposition methods in improving the tribological properties has been reported in different materials.[7,12,45,46] In the present study, the magnitude of the compressive residual stress induced by laser peening is 605 MPa and it is expected to contribute towards the improvement in the fretting wear resistance. The laser peened sample
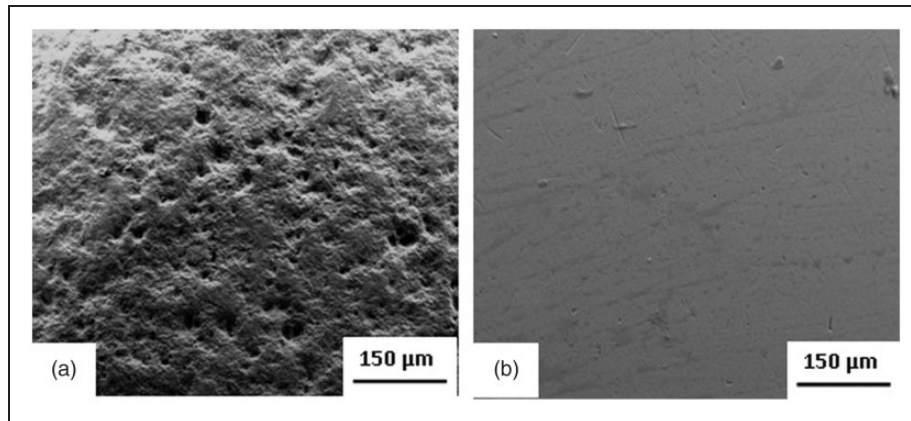
Figure 10. Surface appearance of counterbody material: (a) alumina and (b) steel.
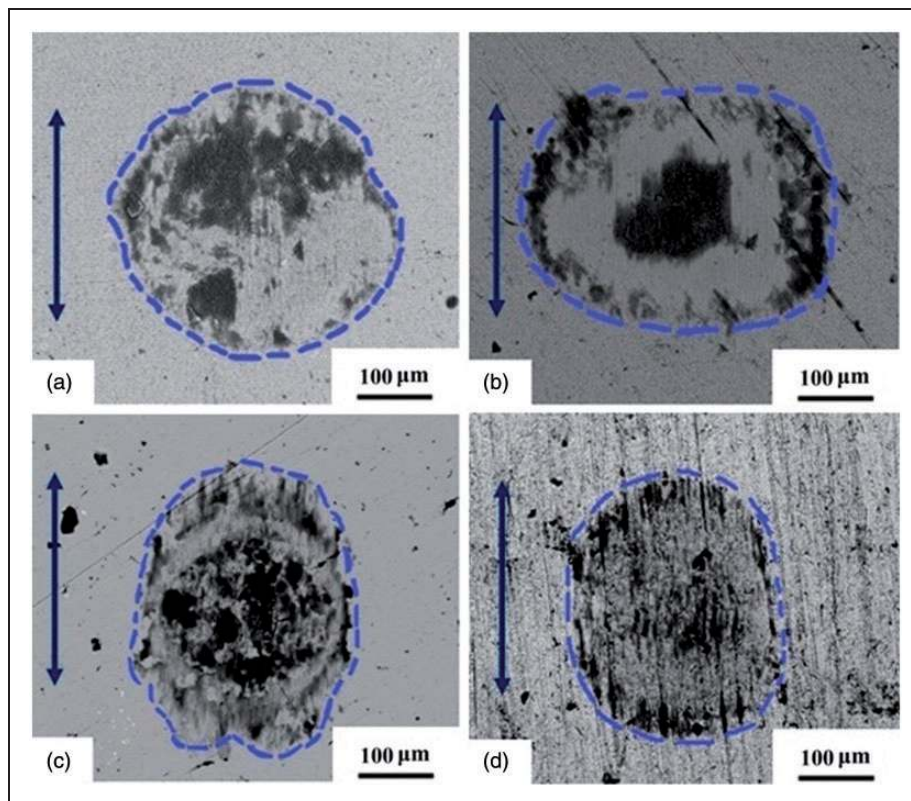

Figure 11. Appearance of fretting wear scars on alloy 718 samples tested at a normal load of 9.8 N: (a) and (c) unpeened; (b) and (d) laser peened; (a) and (b) fretted against alumina ball; (c) and (d) fretted against steel ball. Arrow indicates fretting direction.

exhibited smaller plastic deformation work (refer Figure 6), i.e. higher resistance to plastic deformation and so less possibility of adhesion between the contact surfaces resulting in lower wear rate.

There have been studies on the role of surface roughness on the fretting wear resistance. Rough surfaces are desirable to mitigate fretting wear damage.[40] In the case of rougher surface, the fretting debris at the contact areas may fall into adjacent valleys, may not act as third body abrasive particles, and reduces the abrasive wear resulting in less fretting damage.

In the present study, there is an insignificant increase in R_a value observed after laser peening. Hence, it may be presumed that surface roughness may not have a strong influence on the fretting wear process. A similar observation has been reported in Ti-6Al-4V subjected to USNM treatment.[47]

The wear volume and wear rate of samples fretted against alumina counterbody were higher than those of the samples fretted against steel counterbody. It may be attributed to the tribochemical reaction between alloy 718 and alumina counterbody in

generation of brittle and hard reaction products. Figure 13 shows a scanning electron micrograph of fretting scar on the alumina counterbody fretted against a laser peened alloy 718 sample at a normal load of 1.96 N and the corresponding EDS results. The presence of Ni, Fe and Cr was noted on the worn surface of alumina counterbody indicating material transfer from alloy 718 sample to the alumina counterbody. This implies the probability of forming complex nickel–aluminum intermetallic

oxides such as $NiAl_2O_4$. The reaction between metal oxide and Al_2O_3 produces a complex oxide as shown in equation (4) as suggested by Pepper.[48]

$$NiO + Al_2O_3 \rightarrow NiAl_2O_4 \qquad (4)$$

It is suggested that fracture occurs in the metal rather than at the contact interface having such complex oxides. This leads to material transfer from the
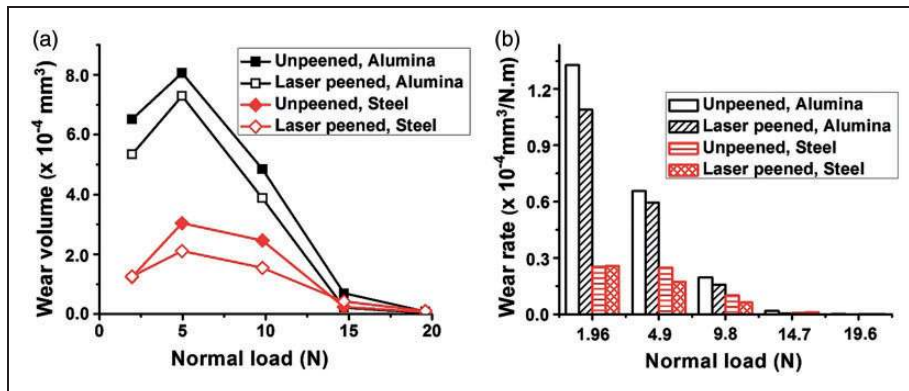

Figure 12. Influence of counterbody material on (a) wear volume and (b) wear rate of alloy 718 samples fretted against alumina and steel counterbodies.
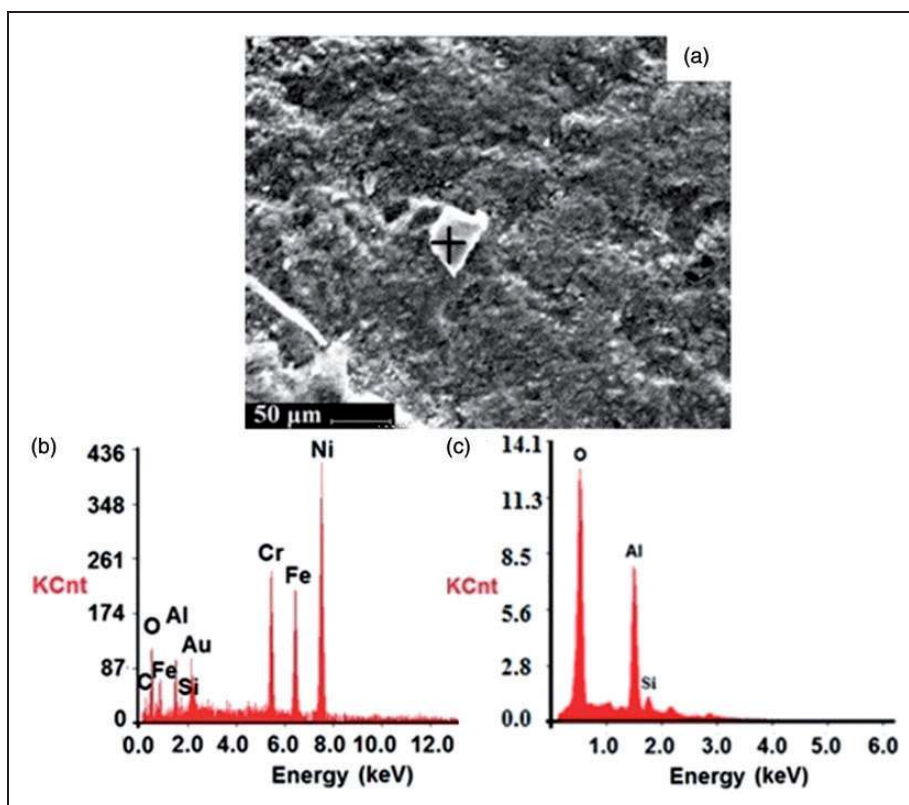

Figure 13. (a) Fretting scar on alumina counterbody fretted against laser peened alloy 718 sample tested at 1.96 N; (b) corresponding EDS result for a region marked ' + ' in (a); and (c) EDS result for a fresh unfretted alumina counterbody.
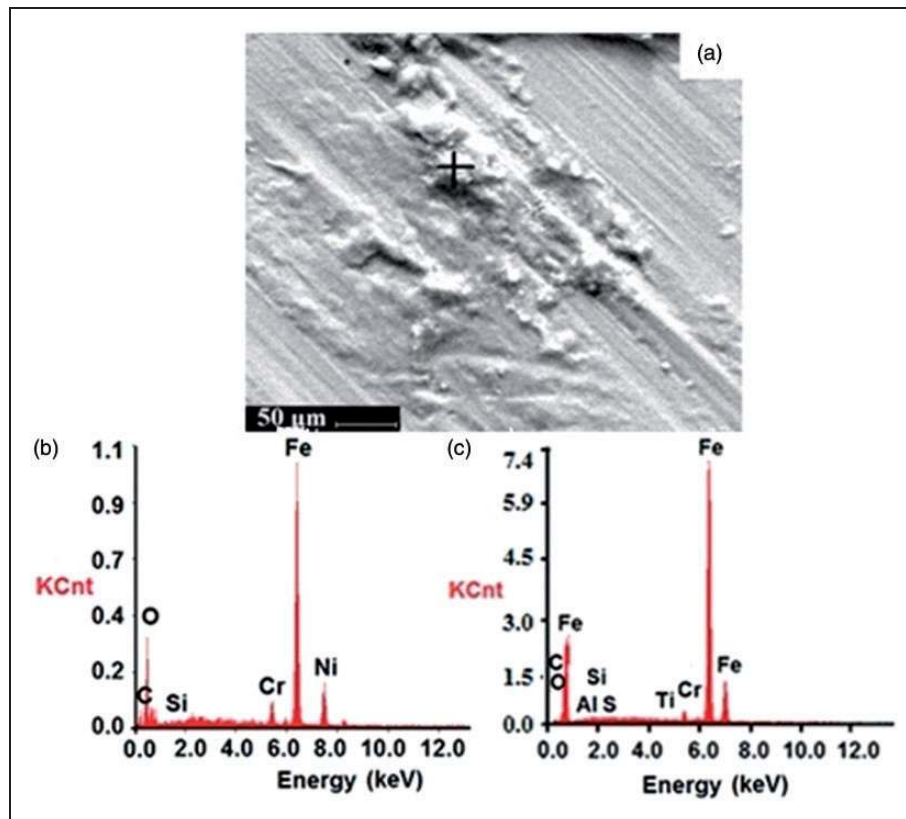
Figure 14. (a) Fretting scar on steel counterbody fretted against laser peened alloy 718 sample tested at 1.96 N; (b) corresponding EDS result for a region marked ' + ' in (a); and (c) EDS result for a fresh unfretted steel counterbody.

sample to the alumina counterbody. This results in higher TFC values and higher wear volume in case of samples fretted against alumina.

However, there was insignificant or no transfer of material from alloy 718 sample to steel counterbody according to EDS results (see Figure 14). Thus, the wear volume of alloy 718 samples fretted against steel counterbody is lower than that of the sample fretted against alumina counterbody. A three-body abrasion wear situation due to the presence of abrasive hard wear debris at the tribo-interface produced by tribochemical reaction between alloy 718 samples and alumina counterbody might have resulted in relatively higher wear volume. Furthermore, it could be seen that at higher normal load (19.6 N), samples fretted against alumina and steel counterbodies exhibited almost similar wear volume and wear rate. It could be attributed to near-stick fretting regime operating at the higher loads. In this regime, the applied displacement is contained by elastic deformation of the asperities resulting in the negligible wear volume and wear rate irrespective of the counterbody used.

Conclusions

Based on the results obtained in the experimental study on laser peening done on alloy 718 and fretting wear tests conducted on laser peened and unpeened samples of alloy 718 fretted against two counterbody materials, the following conclusions are drawn. Laser peening resulted in grain refinement with the formation of nanocrystallites on the surface, increased surface hardness, and compressive residual stress. It did not alter the surface roughness in a significant manner. Owing to higher hardness, adhesion was less and so the tangential force coefficient (TFC) of laser peened samples was less than that of unpeened samples. The samples fretted against alumina counterbody exhibited higher TCF compared to the samples fretted against steel counterbody. This is attributed to higher Hertzian contact stress and tribochemical reactions involved between alloy 718 sample and alumina counterbody. The fretting wear resistance of laser peened samples was superior to that of unpeened samples due to favourable properties exhibited by the laser peened samples, viz. higher surface hardness, lower TFC and higher compressive residual stress. The samples fretted against alumina counterbody suffered more fretting damage compared to the samples fretted against steel counterbody. This is attributed to tribochemical reactions between alloy 718 and alumina counterbody in generation of brittle and hard reaction products.

References

1. Smith WF. *Structure and properties of engineering alloys*. 2nd ed. New York, NY: McGraw-Hill Inc, 1993, p.498.

2. Erdemir and Fenske GR. *Wear resistance of metals and alloys*. Chicago, IL: ASM International, 1988, p.89.

3. Hoeppner DW. In: M Helmi Attai and RB Waterhouse (eds) *Mechanisms of fretting-fatigue and their impact on test methods development*, Standardization of Fretting Fatigue Test Methods and Equipment. Philadelphia, PA: ASTM STP 1159, 1992, pp.23–32.

4. Waterhouse RB. *Fretting fatigue*. 1st ed. London, UK: Applied Science Publishers, 1981.

5. Sequera A, Fu CH, Guo YB, et al. Surface integrity of Inconel 718 by ball burnishing. *J Mat Eng Perf* 2014; 23: 3347–3353.

6. Nabah BAA, Hassan WT, Ryan D, et al. The effect of hardness on eddy current residual stress profiling in shot-peened nickel alloys. *J Nondestruct Eval* 2010; 29: 143–153.

7. Amanov A, Pyun YS, Qingyuan W, et al. Fine grain structure as palliatives for fretting wear of Inconel 718 alloy at various temperatures. In: *8th International symposium on superalloy 718 and derivatives*, Pennsylvania, PA, 28 September–1 October 2014. John Wiley & Sons, New Jersey, pp.555-562.

8. Kumar S, Sudhakar Rao G, Chattopadhyay K, et al. Effect of surface nanostructure on tensile behaviour of superalloy IN718. *Mater Des* 2014; 62: 76–82.

9. Chen T, John H, Xu J, et al. Influence of surface modifications on pitting corrosion behaviour of nickel-base alloy 718. Part 1: effect of machine hammer peening. *Corr Sci* 2013; 77: 230–245.

10. Kamal S, Jayaganthan R and Prakash S. Mechanical and microstructural characteristics of detonation gun sprayed NiCrAlY + 0.4 wt% CeO_2 coatings on superalloys. *Mater Chem Phys* 2010; 122: 262–268.

11. Pichon CL, Cormier J, Dubois JB, et al. Plasma assisted nitriding of Ni-based superalloys with various microstructures. *Surf Coat Tech* 2013; 235: 318–325.

12. Anand Kumar S, Ganesh Sundara Raman S, Sankara Narayanan TSN, et al. Fretting wear behaviour of surface mechanical attrition treated alloy 718. *Surf Coat Tech* 2012; 206: 4425–4432.

13. Kim HD, Kayumov R, Amanov A, et al. Rotary bending fatigue and seizure characteristics of Inconel 718 alloy after ultrasonic nanocrystal surface modification (UNSM) treatment. In: *8th International symposium on superalloy 718 and derivatives*, Pennsylvania, PA, 28 September–1 October 2014. NJ: John Wiley & Sons, p 483-489.

14. Singh V and Meletis EI. Synthesis, characterization and properties of intensified plasma-assisted nitrided superalloy Inconel 718. *Surf Coat Tech* 2006; 201: 1093–1101.

15. Hirschmann ACO, Silva MM, Neto CM, et al. Surface modification of Inconel 718 superalloy by plasma immersion ion implantation. In: *7th International symposium on superalloy 718 and derivatives*, Pennsylvania,

16. Kovacı H, Ghahramanzadeh H, Albayrak Ç, et al. Wear properties of plasma nitrided Inconel 718 superalloy. In: *13th International conference on plasma surface engineering*, Garmisch-Partenkirchen, Germany, 10–14 September 2012, pp.333-337.

17. Nalla RK, Altenberger I, Noster U, et al. On the influence of mechanical surface treatments-deep rolling and laser shock peening on the fatigue behaviour of Ti-6A-4V at ambient and elevated temperatures. *Mater Sci Eng A* 2003; 355: 216–230.

18. Peyre P, Fabbro R, Merrien P, et al. Laser shock processing of aluminium alloys: Application to high cycle fatigue behaviour. *Mater Sci Eng A* 1996; 210: 102–113.

19. Zhou L, Li YH, He WF, et al. Laser shock processing of Ni-base superalloy and high cycle fatigue properties. *Mater Sci Forum* 2012; 697-698: 235–238.

20. He W, Li Y, Li Q, et al. The effects of laser shock peening on fatigue life in Ni-based superalloy. *Adv Mater Res* 2010; 135: 209–214.

21. Forget P, Jeandin M and Lyoret A. Determination of laser shock treatment conditions for fatigue testing of Ni-based superalloys. *J De Phy* 1993; 3: 921–927.

22. Prevey S. The effect of cold work on the thermal stability of residual compression in surface enhanced IN718. In: *Proceedings 20th ASM materials solution conference exposition*, Missouri, October 2000.

23. Montross CS, Wei T, Ye L, et al. Laser shock processing and its effects on microstructure and properties of metal alloys: a review. *Int J Fat* 2002; 24: 1021–1036.

24. Sundar R, Kumar H, Kaul R, et al. Studies on laser peening using different sacrificial coatings. *Surf Eng* 2012; 28: 564–568.

25. Ganesh P, Sundar R, Kumar H, et al. Studies of laser peening on spring steel for automotive applications. *Optics Laser Eng* 2012; 50: 678–686.

26. Cullity BD. *Elements of X-ray diffraction*. Menlo Park, CA: Addison-Wesley, 1978.

27. Noyan IC and Cohen JB. *Residual stress*. New York, NY: Springer-Verlag, 1987.

28. Ramesh R and Gnanamoorthy R. Development of a fretting wear test rig and preliminary studies for understanding the fretting wear properties of steels. *Mater Des* 2006; 27: 141–146.

29. Kalin M and Vizintin J. Use of equations for wear volume determination in fretting experiments. *Wear* 2000; 237: 39–48.

30. Johnson KL. *Contact mechanics*. Cambridge, UK: Cambridge University Press, 2003.

31. Gill A, Telang A, Mannava SR, et al. Comparison of mechanisms of advanced mechanical surface treatments in nickel-based superalloy. *Mater Sci Eng A* 2013; 576: 346–355.

32. He W, Li Y, Nie X, et al. A study of the microstructure and hardness of Ti-5Al-2Sn-2Zr-4Mo-4Cr by laser shock peening. *Appl Mech Mater* 2011; 84: 471–475.

33. Bugayev AA, Gupta M and Payne R. Laser processing of Inconel 600 and surface structure. *Optics Laser Eng* 2006; 44: 102–111.

34. Lu JZ, Luo KY, Zhang YK, et al. Grain refinement of LY2 aluminum alloy induced by ultra-high plastic strain during multiple laser shock processing impacts. *Acta Mater* 2010; 58: 3984–3994.

35. Lu JZ, Luo KY, Zhang YK, et al. Grain refinement mechanism of multiple laser shock processing impacts on AISI 304 stainless steel. *Acta Mater* 2010; 58: 5354–5362.

36. Anand Kumar S, Sundar R, Ganesh Sundara Raman S, et al. Fretting wear behaviour of laser peened Ti-6Al-4V. *Tribol Trans* 2012; 55: 615–623.

37. Tao NR, Wang ZB, Tong WP, et al. An investigation of surface nanocrystallization mechanism in Fe induced by surface mechanical attrition treatment. *Acta Mater* 2002; 50: 4603–4616.

38. Zhu L, Xu B, Wang H, et al. Effect of residual stress on the nanoindentation response of (100) copper single crystal. *Mater Chem Phys* 2012; 136: 561–565.

39. Mordyuk BN and Prokopenko GI. Ultrasonic impact peening for the surface properties' management. *J Sound Vibrat* 2007; 308: 855–866.

40. Fu Y, Wei J and Batchelor AW. Some considerations on the mitigation of fretting damage by the application of surface-modification technologies. *J Mater Proc Tech* 2000; 99: 231–245.

41. Zhang YS, Han Z, Wang K, et al. Friction and wear behaviours of nanocrystalline surface layer of pure copper. *Wear* 2006; 260: 942–948.

42. Mubarak Ali M, Ganesh Sundara Raman S, Pathak SD, et al. Fretting wear behaviour of plasma nitrided Ti–6Al–4V fretted against unnitrided Ti–6Al–4V and alumina counterbodies. *Trans Ind Inst Met* 2009; 62: 59–64.

43. Vingsbo O and Soderberg S. On fretting maps. *Wear* 1988; 126: 131–147.

44. Labedz J. Metal treatments against wear, corrosion, fretting fatigue. In: RB Waterhouse and A Niku-Lari (eds) *Effect of residual stresses on wear of the surface layer of components operating under fretting conditions*. Pergamon Press, Oxford, 1988, pp.87–98.

45. Horswill NC, Sridharan K and Corad JR. A fretting wear study of a nitrogen implanted titanium alloy. *J Mater Sci Lett* 1995; 14: 1349–1351.

46. Waterhouse RB. The effect of surface treatments on the fretting wear of an aluminum alloy/steel couple. *Wear* 1982; 68: 310–334.

47. Amanov A, Cho IS, Kim DE, et al. Fretting wear and friction reduction of CP titanium and Ti–6Al–4V alloy by ultrasonic nanocrystalline surface modification. *Surf Coat Tech* 2012; 207: 135–142.

48. Pepper SV. Effect of adsorbed films on friction of Al2O3-metal systems. *J Appl Phys* 1976; 47: 2579–2583.